Effect of Laser Power and Travel Speed on the Welding Process and Tensile Strength of Rolled Zinc Alloy Laser Welds*

Lena Golda
Faculty of Mechanical and Medical Engineering, Furtwangen University (HFU), 2022

***Abstract*— For thin zinc sheets for construction purposes different welding techniques like tungsten inert gas (TIG), plasma arc (PAW) or micro-friction stir (µFSW) welding can be used. However, low ultimate tensile strength (UTS) often leads to cracking in the weld even at low loads. The characteristics of laser welding make it particularly suitable for joining thin sheets and low-melting materials. Nevertheless, little is known about the weldability of thin zinc sheets by laser welding and the effects of the basic process parameters of laser power and travel speed on the welding process and the UTS of the weld. In this study, thin zinc sheets were welded at different laser powers and travel speeds. Tensile testing of the welded joint showed, that the UTS and elongation at break increase with the energy input per unit length, but the welding process became gradually unstable and the susceptibility for welding defects increased. This leaves only a few laser powers and travel speeds that produce good welds with respect to UTS and elongation at break. Under these conditions laser welding is an alternative processing technique to TIG, PAW and µFSW, but needs further investigation to improve its stability. To implement laser welding in highly automated production processes further research is required on laser welding of rolled zinc alloys.**

Keywords - Laser Welding, Zn-Cu-Ti, Zinc, Titan Zinc, Thin Metal Sheets, Tensile Testing, Metal Pipes Production

I. Introduction

Zinc alloys are often used in the construction industry, e. g. for roofing materials, facades, and roof drainage systems. When rolled zinc alloys are welded for construction purposes, low tensile strength and brittleness often lead to cracking within the weld zone even at low loads [1]. Pantazopoulos and Sampani investigated weld failures of rolled zinc alloy strips and tubes [2, 3]. They associated the fracture of the welded tube with microfissures in the weld joint, which also significantly reduced the ductility and formability of the tubing and result in an almost brittle weld fractur. They also found various welding defects in the weld of the strip such as linear discontinuities, edge microcracks and gas porosity. Although rolled zinc alloys are being joined in the industry not only by TIG but also by PAW, no results have so far been published on this subject. Papaefthymiou et al. and Galvão et al. studied µFSW of rolled zinc alloys [1, 4]. Galvão et al. found defects in the weld such as kissing bonds and cracks in the root leading to poor tensile performance and brittleness. Papaefthymiou et al. compared µFSW of thin zinc sheets with TIG welds. Welding 700 µm thick sheets they found kissing bond defects weakening the weld. A thinning of the material by 15% further weakened the material's resistance. Nevertheless, the tensile strength of the µFSW welds was only 30 N/mm^2 lower than the tensile strength of the TIG welds.

Laser welding offers advantageous characteristics for joining thin sheets of low-melting materials such as a small heat-affected zone, low thermal alteration of the material, and low distortion, which also benefits particularly long seams. Further advantages are easy automation, high process speeds, good repeatability, and a visually appealing narrow bead. However, no research has been published on laser welding of rolled zinc alloys. Laser welding is categorized into conduction and deep penetration (keyhole) welding. In conduction mode welding, the laser energy is coupled into the material surface and transferred into the material by heat conduction. The laser power density does not cause boiling of the melt pool and the evaporation rate is insignificant resulting in a very stable welding process. Most of the laser power is reflected resulting in shallow welds with a low aspect ratio, defined as the ratio of the penetration depth to the bead width. In keyhole mode, the high laser power density not only melts the material, but also vaporizes it at a high evaporation rate. The intense vaporization causes a sharp increase in vapor pressure (recoil pressure), which forces a hole in the melt pool and forms a capillary (keyhole). Due to the keyhole, significantly more energy can be coupled into the material. This results in welds with high aspect ratios. [5, 6] A third mode, the unstable or transition mode, was observed between the conduction and keyhole welding regimes [6].

Aalderink et al. and Eriksson et al. have observed a phenomenon that occurs exclusively in keyhole welding of thin sheets and can lead to weld defects [7, 8]. For laser welds in sheets thicker than 3 mm, the width of the welds is usually less than their depth. The keyhole is kept open by the evaporation pressure on the capillary wall, which counteracts the surface tension forces trying to close the keyhole. For laser welds in thinner sheets, the width of the welds is greater than their depth. This can cause the surface tension forces to hold the keyhole open, resulting in weld defects. [7]

This paper investigates the influence of laser power and travel speed on the welding process and UTS of rolled zinc alloy welds. For this purpose, a rolled zinc alloy was welded at laser powers from 300 to 2100 W and travel speeds between 3 and 7 m/min. The welding process was evaluated through high-speed camera footage. The welded samples were visually inspected and examined through tensile testing. The objective of this study is to verify the laser weldability of rolled zinc alloys and to determine the optimum welding speed and laser power settings.

*This research has been supported by professor Hadi Mozaffari-Jovein (HFU), Grömo GmbH & Co. KG, Laserline GmbH and SEKO – Technologie + Service GmbH

II. Materials and Methods

A. Sample Preparation

The material used was a 0.65 mm thick rolled zinc alloy designated as alloy EN 988 : 1996 by the European standard. Its chemical composition is displayed in Table 1.

Table 1: Chemical Composition of zinc alloy EN 988 : 1996 [9]

Chemical Composition in Percentage by Mass				
	Cu	Ti	Al	Zn[1]
EN 988	0.08-1.0	0.06-0.2	≤ 0.015	balance

[1] *Zinc grade Z1 according to EN 1179, i.e., with a zinc content of at least 99.995% under addition of alloying elements*

The 500 mm long welds were produced using a Laserline diode laser LDF 6000-40 and an OTS3 optic with a 1.27 mm laser spot diameter. Continuous welding was applied. The laser was tilted by 15°. To shield the welding area Argon 4.6 was supplied coaxially to the weld. The resulting vapors were extracted. The metal sheets were butt-welded. The diode laser welding process of the thin zinc sheets was recorded by a Photron FASTCAM Mini high-speed camera to capture the influence of travel speed and laser power variations on den welding process.

The metal sheets are prepared for the welding process as follows:

1. The sheet edges are honed on both sides.
2. The sheet is bent into a pipe.
3. The sheet edges are cleaned with petroleum ether.
4. The sheet edges are positioned to a butt joint.

In the first set of experiments, travel speeds between 3 and 7 m/min were applied. The laser power was varied between 300 and 1800 W.

In the second set of experiments, travel speeds of 6 and 7 m/min were applied at laser powers ranging from 1000 W to 2100 W.

B. Measurement Setup

In the first set of experiments, all samples were tested non-destructively by visual inspection. Weld defects and other characteristics of the weld were examined and matched with the video footage of the high-speed camera. The welding mode was determined by detecting the three states of the melt pool on the high-speed camera images: no boiling of the melt pool (conduction mode), boiling of the melt pool (unstable mode), and the formation of a stable keyhole (keyhole mode).

In the second set of experiments, five specimens of each parameter set were tested through destructive testing transverse to rolling direction of the zinc alloy. The tensile test was performed on a tensile testing setup by ZwickRoell according to DIN EN ISO 6892-1. The specimen for tensile testing is shown in Figure 1. The mean value and standard deviation of the results were determined statistically.

Figure 1: Specimen for Tensile Testing ISO6892-1 B.1-1 12.5 × 60

III. Results

A. Welding Process

The welding modes are distinguished by the boiling of the melt pool and keyhole formation, which was observed on the high-speed camera footage. Which welding mode takes place is strongly influenced by which laser power is used at which travel speed, i.e. which energy is applied over a given distance. The energy input per unit length E_{ul} is calculated by dividing the *laser power P* by the *travel speed v*:

$$E_{ul} = \frac{P}{v}[J/cm] \quad (1)$$

At energy inputs per unit length between 60 and 120 J/cm conduction mode welding was observed. Individual bubbles did rise, but the melt pool was calm most of the time and did not boil (see Figure 2). The welding process was stable and produced mostly superficially sound welds. However, the welds had a small and inconsistent root width. With increasing E_{ul}, the melt pool became gradually unstable. From 120 J/cm boiling of the melt pool as depicted in Figure 3 occurred periodically. In this unstable welding mode, the melt pool alternated between a boiling and a calm state and rarely keyhole formation and waves on the melt pool were observed. From 140 J/cm the melt pool boiled continuously. In Figure 4 the formation and immediate collapse of a keyhole as well as the resulting welding defect at 140 J/cm is depicted. As the E_{ul} continued to increase, the welding mode became more unstable, boiling intensified, and the formation of keyholes was more likely. Keyholes began to elongate before collapsing. Figure 5 shows the formation, elongation, and collapse of a keyhole at 170 J/cm and the resulting faulty weld.

Figure 2: Weld during (left) and after (right) conduction mode laser welding at 110 J/cm (700 W, 4 m/min) with a calm melt pool

Figure 3: Weld during (left) and after (right) laser welding at 120 J/cm (800 W, 4 m/min) with a boiling melt pool

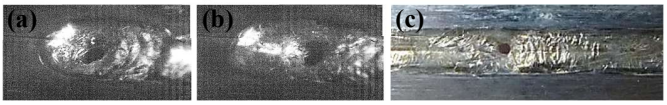

Figure 4: Keyhole Formation (a) and immediate collapse (b) at 140 J/cm (900 W, 4 m/min) and the resulting welding defect (c)

Figure 5: Keyhole formation (a) and elongation (b) at 170 J/cm (1100 W, 4 min/m) and the resulting welding defect (c)

Even with an E_{ul} of more than 180 J/cm, it was not possible to maintain a stable keyhole, so that welding in keyhole mode could not be applied.

At travel speeds of 3 to 5 m/min, the welding process was very susceptible to welding defects even at E_{ul} < 120 J/cm These defects were caused by bigger bubbles of zinc vapor leaving the

melt pool. At travel speeds of 6 and 7 m/min the process was more stable. Defects due to keyhole formation and collapse occurred regularly only at an E_{ul} of at least 180 J/cm.

It was observed that weld width decreased slightly while welding speed increased. At 3 m/min the weld was 1.9 mm wide. At 7 m/min the weld width was 1.7 mm. Figure 6 shows the weld seams and roots generated at 6 m/min travel speed. When conduction welding was applied the seam was smooth and raised in relation to the sheet surface at E_{ul} = 100 J/cm and relatively flat at E_{ul} = 120 J/cm. In unstable mode (E_{ul} > 120 J/cm) V-shaped striations (chevron pattern) appeared on the weld surface as well as grooves at the edge of the welding seam. With increasing E_{ul}, the grooves became deeper, and the root sag and root width increased. Root width deviations were found in all welds.

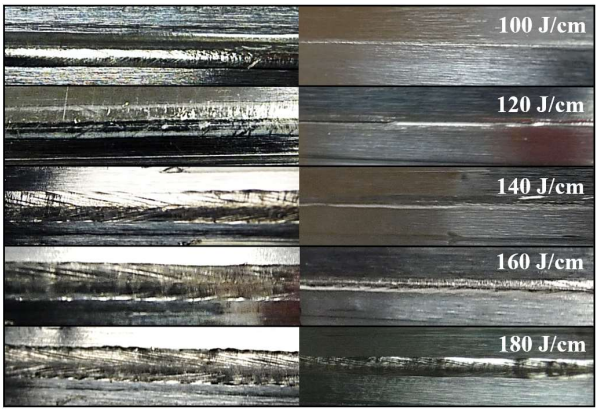

Figure 6: Seam (left) and root (right) of the welds at 6 m/min

B. Ultimate Tensile Strength

In Figure 7 the stress-strain diagrams of the welds at 6 m/min and 7 m/min travel speed and an E_{ul} from 100 J/cm to 180 J/cm are presented. Figure 8 shows the stress-strain diagram of the rolled zinc alloy on the left and a bar graph of all tensile test results on the right. Table 2 shows the process parameters and the determined ultimate tensile strengths. The UTS increased with increasing E_{ul} and its standard deviation (SD) decreased. The elongation at break (A%) of the specimens also increased with increasing E_{ul}. The welds at 100 J/cm had a low average UTS of 113.3 N/mm^2 at 6 m/min and 171.1 N/mm^2 at 7 m/min and an very high SD of UTS (79.1 and 56.6). The weld at 120 J/cm and 7 m/min had an even lower average UTS of 84.3 N/mm^2. At 120 J/cm all specimens had a very low elongation at break of 0.5 and 0.3 %. The highest average UTS of 221.0 N/mm^2 with the lowest SD of UTS of 1.9 and the largest elongation at break of 3.7 % were obtained at 180 J/cm and 7 m/min. Overall the specimens at 7 m/min had a slightly higher elongation at break than the specimens at 6 m/min, but the ultimate tensile strength was comparable.

IV. DISCUSSION

A. Welding Process

The high-speed camera's recordings and findings of the visual inspection confirm an unstable mode between the conduction and keyhole mode as reported by Katayama [6]. In unstable mode the melt pool is boiling. There is a probability of keyhole formation and immediate collapse. Keyhole mode could not be applied because even with sufficient laser power density, the keyholes elongated and collapsed almost immediately after their formation. The instability of the keyhole can be explained by the theory proposed by Eriksson et al. and Aalderink et al., according to which this phenomenon is caused by surface tension effects occurring in thin metal sheets (< 3 mm) [7, 8]. Eriksson et al. state, that the ratio of melt pool width to melt pool thickness should be less than 1.5 to avoid this behavior. Although Aalderink et al. mention a material dependence of this ratio, the ratios of 2.62 to 2.92 occurring in the experimental setup of this research make the presence of these unfavorable surface tension effects very likely.

The travel speed not only influences which welding mode takes place, but also seems to influence the melt pool stability. With longer laser-material interaction time the risk of bigger bubbles emerging from the melt pool as well as keyhole formation and collapse increased. This caused the welding process to be generally more unstable and prone to weld defects at lower travel speeds ($v \leq 5$ m/min). At travel speeds from 6 m/min the welding process stabilized. Even when the melt pool was continuously boiling ($E_{ul} \geq 140$ J/cm) holes in the weld were very unlikely. Only at an E_{ul} of 180 J/cm or more the formation and collapse of keyholes regularly resulted in defects.

In conduction mode the melt pool is calm, and the evaporation rate is low. There is no significant recoil pressure, and a smooth surface is generated. The grooves and chevron pattern which are often seen in keyhole mode laser welds [8] were observed in the unstable mode and result from waves on the melt pool caused by recoil pressure and surface tension [10].

Table 2: Results of the Tensile Tests

Laser Power [W]	E_{ul} [J/cm]	Travel Speed [m/min]	UTS Specimen 1 [N/mm^2]	UTS Specimen 2 [N/mm^2]	UTS Specimen 3 [N/mm^2]	UTS Specimen 4 [N/mm^2]	UTS Specimen 5 [N/mm^2]	UTS [N/mm^2]	A [%]	Standard Deviation UTS	Standard Deviation A%
1000	100	6	211.0	166.0	91.1	4.5	94.1	113.3	0.6	79.1	0.6
1200	120	6	132.0	108.0	133.0	171.0	117.0	132.2	0.5	24.0	0.1
1400	140	6	201.0	204.0	172.0	184.0	212.0	194.6	1.2	16.0	0.4
1600	160	6	219.0	216.0	214.0	215.0	213.0	215.4	2.6	2.2	0.5
1800	180	6	218.0	221.0	221.0	218.0	217.0	219.0	3.4	1.9	0.6
1167	100	7	203.0	202.0	189.0	191.0	70.6	171.1	1.2	56.6	0.6
1400	120	7	106.0	59.6	87.7	76.1	92.3	84.3	0.3	17.4	0.1
1633	140	7	213.0	219.0	204.0	177.0	182.0	199.0	1.7	18.7	1.0
1867	160	7	222.0	222.0	222.0	181.0	207.0	210.8	2.7	17.9	1.3
2100	180	7	222.0	223.0	220.0	222.0	218.0	221.0	3.7	1.9	0.7
Rolled Zinc Alloy EN 988 : 1996			233.0	232.0	233.0	232.0	232.0	232.4	19.1	0.6	0.8

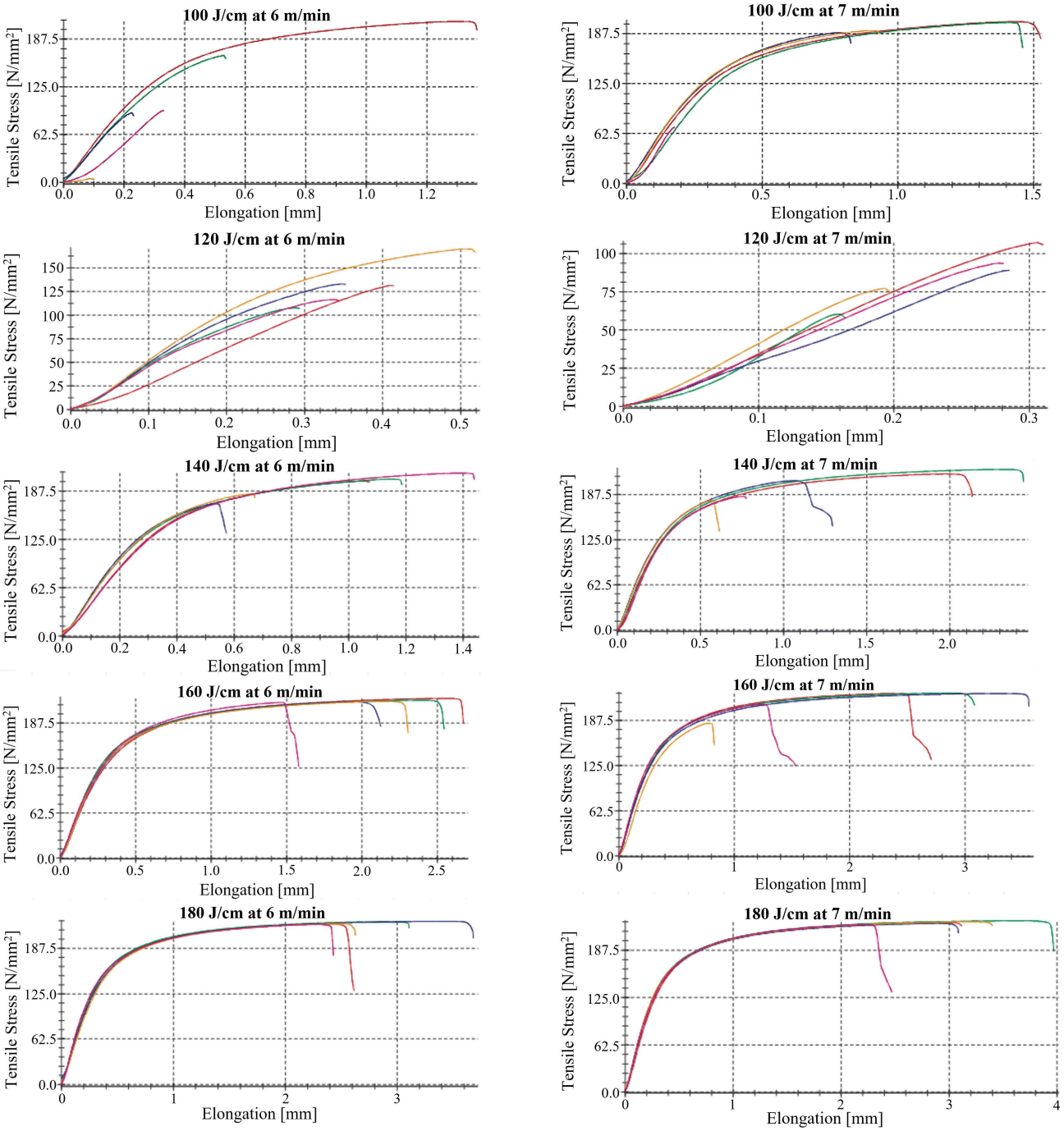

Figure 7: Stress-strain diagrams of the welds at E_{ul} ranging from 100 to 180 J/cm and travel speeds of 6 and 7 m/min

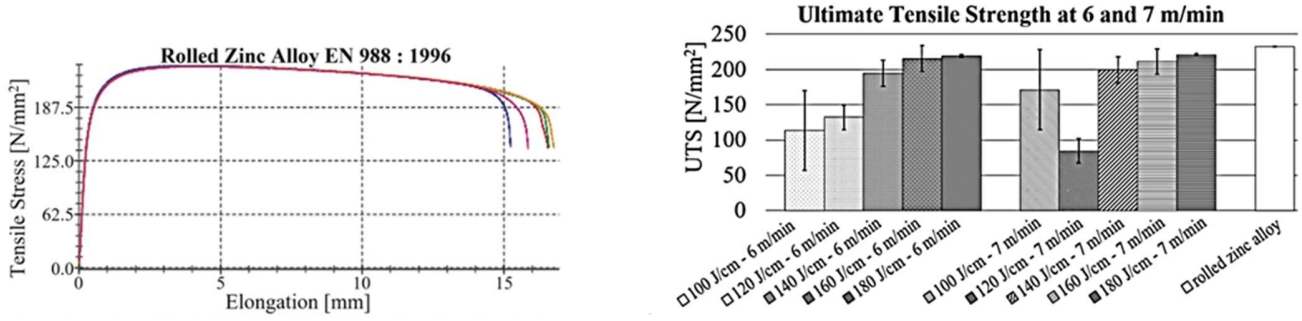

Figure 8: Stress-strain diagram of the rolled zinc alloy (left) and UTS of all welds and the base material (right)

B. *Ultimate Tensile Strength*

At 100 and 120 J/cm, the root width is very thin compared to the welds at 140 to 180 J/cm. Therefore, the root width deviations apparent in all welds might lower the UTS especially at $E_{ul} \leq 120$ J/cm. A higher E_{ul} showed to increase the ultimate tensile strength of the weld, but also the tendency for holes to form due to keyhole formation and collapse increased. At higher travel speeds the welds were overall slightly less brittle with exception of the weld seams at 120 J/cm. The small increase in ductility might be caused by the higher laser powers applied to account for the higher travel speed. The low UTS of the seemingly sound conduction welds and its high SD were likely caused by weld defects, such as microcracks, or porosity, which were found in the work of Pantazopoulos and Sampani [2, 3].

V. CONCLUSION & OUTLOOK

(i) For this paper, a rolled zinc alloy according to EN 988 : 1996 was welded at laser powers from 300 to 2100 W and travel speeds in a range of 3 to 7 m/min. The effect of travel speed and laser power on welding process and ultimate tensile strength (UTS) of the laser welds where examined through high-speed camera recordings, visual inspection, and tensile testing. It was found that significantly lower UTS and lower elongation at break occurred in specimens welded with an energy input per unit length (E_{ul}) of 120 J/cm or less. With increasing E_{ul}, the UTS and the elongation at break increased. At the same time, the welding process became gradually unstable and the susceptibility for holes in the weld increased. This could be determined by the camera recordings and the visual inspection of the welds. At 160 J/cm, welds with a defect-free surface could be obtained with UTS only 15 to 20 N/mm^2 lower than the UTS of the base material, confirming the weldability of thin zinc sheets. However, the welding process of rolled zinc alloys is unstable and could only be applied successfully within a very limited number of laser powers and travel speeds. The welds with the highest UTS and a defect-free surface were obtained at a travel speed of 6 m/min and a laser power of 1600 W.

(ii) From 60 to 120 J/cm conduction mode welding was observed. Welding in conduction regime leads to a smooth and defect-free surface of the weld. Above 120 J/cm, an unstable welding mode was observed, in which the melt pool boiled and the probability of formation and immediate collapse of keyholes leading to weld defects was increased.

(iii) Keyhole mode could not be applied successfully when welding the rolled zinc alloy due to unfavorable surface tension effects.

(iv) At higher travel speeds of 6 to 7 m/min the laser welding process was more stable and less susceptible to the formation of holes in the weld, than at lower travel speeds of 3 to 5 m/min.

(v) The UTS increased with increasing E_{ul} and the standard deviation of UTS decreased. The elongation at break (A%) also increased with increasing E_{ul} as well as with higher travel speeds.

(vi) Conduction mode welding ($E_{ul} \leq 120$ J/cm) is recommended to achieve a stable welding process. However, the UTS and elongation at break of the conduction mode welds were not satisfactory. In unstable mode, the UTS and elongation at break of the welds were satisfactory, but the process was very susceptible to the formation of holes in the weld. This leads to two possible approaches: The causes of the low UTS could be investigated by microscopic examination and countermeasures identified. Alternatively, the unstable regime could be further stabilized, e.g. by welding at higher process speeds ($v > 7$ m/min).

(vii) This work has provided fundamental knowledge about laser welding of rolled zinc alloys and provides a basis for further investigation and optimization of the laser welding process. With the implementation of laser welding rolled zinc alloys in the construction industry, production processes can be automated further and become more efficient.

VI. REFERENCES

[1] S. Papaefthymiou, C. Goulas und E. Gavalas, „Micro-friction stir welding of titan zinc sheets“, *Journal of Materials Processing Technology*, Jg. 216, S. 133–139, 2015, doi: 10.1016/j.jmatprotec.2014.08.029.

[2] G. Pantazopoulos und A. Sampani, „Analysis of a weld failure of a rolled Zn-alloy strip – A case study“, *Engineering Failure Analysis*, Jg. 14, Nr. 4, S. 642–651, 2007, doi: 10.1016/j.engfailanal.2006.03.005.

[3] G. Pantazopoulos und A. Sampani, „Microstructure and failure of a welded ZnTiCu tube“, *J. Fail. Anal. Preven.*, Jg. 5, Nr. 5, S. 16–19, 2005, doi: 10.1361/154770205X65954.

[4] I. Galvão, C. Leitão, A. Loureiro und D. Rodrigues, „Friction Stir Welding of very thin plates“, *Soldag. insp.*, Jg. 17, Nr. 1, S. 2–10, 2012, doi: 10.1590/S0104-92242012000100002.

[5] J. Svenungsson, I. Choquet und A. F. Kaplan, „Laser Welding Process – A Review of Keyhole Welding Modelling“, *Physics Procedia*, Jg. 78, S. 182–191, 2015, doi: 10.1016/j.phpro.2015.11.042.

[6] S. Katayama, *Handbook of laser welding technologies*. Sawston, Cambridge, UK: Woodhead Publishing Limited, 2013.

[7] I. Eriksson, J. Powell und A. F. H. Kaplan, „Surface tension generated defects in full penetration laser keyhole welding“, *Journal of Laser Applications*, Jg. 26, Nr. 1, S. 12006, 2014, doi: 10.2351/1.4830175.

[8] B. J. Aalderink, D. F. de Lange, R. G. K. M. Aarts und J. Meijer, „Keyhole shapes during laser welding of thin metal sheets“, *J. Phys. D: Appl. Phys.*, Jg. 40, Nr. 17, S. 5388–5393, 2007, doi: 10.1088/0022-3727/40/17/057.

[9] *Zinc and zinc alloys - Specification for rolled flat products for building*, DIN EN 988:1996, German Institute for Standardization, 00.Aug. 1996.

[10] A. Matsunawa und V. Semak, „The simulation of front keyhole wall dynamics during laser welding“, *J. Phys. D: Appl. Phys.*, Jg. 30, Nr. 5, S. 798–809, 1997, doi: 10.1088/0022-3727/30/5/013.